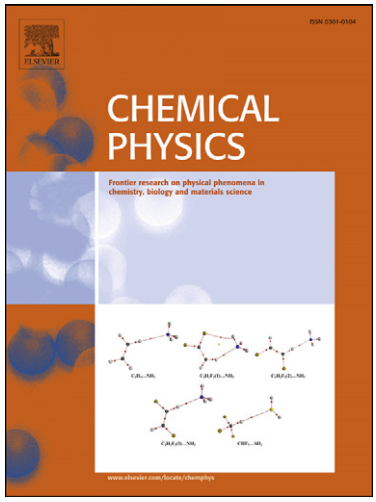

Intermolecular potentials for simulations of collisions of $SiNCS^+$ and $(CH_3)_2SiNCS^+$ ions with fluorinated self-assembled monolayers

Juan José Nogueira, Antonio Sanchez-Coronilla, Jorge M.C. Marques, William L. Hase, Emilio Martínez-Núñez, Saulo A. Vázquez

PII: S0301-0104(11)00074-7
DOI: 10.1016/j.chemphys.2011.02.014
Reference: CHEMPH 8144

To appear in: *Chemical Physics*

Received Date: 14 January 2011
Accepted Date: 24 February 2011

Please cite this article as: J.J. Nogueira, A. Sanchez-Coronilla, J.M.C. Marques, W.L. Hase, E. Martínez-Núñez, S.A. Vázquez, Intermolecular potentials for simulations of collisions of $SiNCS^+$ and $(CH_3)_2SiNCS^+$ ions with fluorinated self-assembled monolayers, *Chemical Physics* (2011), doi: 10.1016/j.chemphys.2011.02.014

Intermolecular potentials for simulations of collisions of $SiNCS^+$ and $(CH_3)_2SiNCS^+$ ions with fluorinated self-assembled monolayers

Juan José Nogueira,[a] Antonio Sanchez-Coronilla,[a,1] Jorge M.C. Marques,[b] William L. Hase,[c,*] Emilio Martínez-Núñez,[a,*] and Saulo A. Vázquez[a,*]

[a]Departamento de Química Física y Centro Singular de Investigación en Química Biológica y Materiales Moleculares, Universidad de Santiago de Compostela, 15782 Santiago de Compostela, Spain

[b]Departamento de Química, Universidade de Coimbra, 3004-535 Coimbra, Portugal

[c]Department of Chemistry and Biochemistry, Texas Tech University, Lubbock, Texas 79409

*Corresponding authors: bill.hase@ttu.edu, Emilio.nunez@usc.es, and saulo.vazquez@usc.es

Abbreviations: self-assembled monolayer (SAM), density functional theory plus dispersion (DFT-D), intermolecular potential energy curves (IPECs), basis set superposition error (BSSE)

[1] Present address: Centro de Química Estrutural, Complexo 1, Instituto Superior Técnico, Avenida Rovisco Pais, 1049-001 Lisboa, Portugal

Abstract

Analytical potential energy functions were developed for interactions of $SiNCS^+$ and $(CH_3)_2SiNCS^+$ ions with perfluorinated self-assembled monolayer (F-SAM) surfaces. Two model compounds were used to represent an F-SAM: CF_4 and nine chains of perfluorobutane forming a miniSAM structure. Density functional theory plus dispersion (DFT-D) calculations were carried out to compute intermolecular potential energy curves (IPECs) for these systems. The applied DFT-D method (specifically, B97-D) was successfully tested against high-level wavefunction calculations performed on the smallest system investigated. The IPECs calculated at the B97-D level were fitted to analytical potentials of the Buckingham type. The calculations show that the parameters obtained from the fits involving CF_4 are transferable to the miniSAM system, provided the fittings are conducted with caution, thus corroborating that CF_4 is a good model for parameterizing intermolecular potentials for interactions of gases with F-SAM surfaces.

Key words: silyl ions, perfluorinated self-assembled monolayer, intermolecular potential energy curves, analytical potentials, density functional theory plus dispersion (DFT-D)

1. Introduction

More than one decade ago, Cooks and co-workers [1] described a method for preparing modified surfaces, in which intact polyatomic ions were deposited from the gas phase onto a self-assembled monolayer surface of fluorinated alkanethiols, $CF_3(CF_2)_7(CH_2)_2SH$, on a polycrystalline gold surface (F-SAM). This intact deposition of projectile ions impinging on surfaces at low collision energies (<100 eV) was referred to as soft-landing, and this process may occur with or without retention of the initial ion charge [2-4]. Experiments of soft-landing have involved a wide variety of projectile ions, including small and medium-size polyatomic ions [1,5-12], clusters [13-24], peptides [11,23,25-30], proteins [25,31,32], a nucleotide [33], and intact viruses [34,35]. SAMs were used in many of these experiments because their well-characterized structure, controllable surface properties and biocompatibility make them convenient targets for biological and medical applications [36].

Collisions of polyatomic ions with surfaces may lead to several physical and chemical processes that compete with soft-landing [3]. Examples are inelastic scattering of the projectile ion, surface-induced dissociation (SID), and reactive landing resulting in covalent modification of the surface. Experimental observations show that the efficiencies of these competing processes depend on the nature of the ion, the physical and chemical properties of the surface, the collision energy, and the incident angle. Soft-landing takes place when the amount of translational energy of the projectile ion that is transferred to the surface and to the internal degrees of freedom of the ion is such that there is insufficient recoil translational energy for the ion to escape from the surface attraction.

Silyl ions are among the smallest projectile ions selected by Cooks and co-workers for experiments of soft-landing [1,5,12]. They observed soft-landing for $(CH_3)_2SiNCS^+$, but not for the lighter H_2SiNCS^+ and $SiNCS^+$ ions, and found evidences that the $(CH_3)_2SiNCS^+$ projectiles trapped in the monolayer retain the charge. The analysis of the accumulated data for various classes of compounds led Cooks and co-workers to conclude that successful soft-landing of polyatomic ions is favored by relatively bulky steric groups. The inclusion of methyl groups in the silyl ion can be expected to increase the attractive intermolecular interaction with the monolayer, and may also facilitate entrapment of the ion within the F-SAM chains [1,5].

Trajectory chemical dynamics simulations provide a valuable complement to experimental determinations, as they allow for the study of certain features that may be difficult, if not unfeasible, to be explored by experiment. Actually, classical trajectory calculations have been successfully employed for the investigation of the dynamics of energy transfer of collisions of gases, including protonated peptide ions, with self-assembled monolayers [37-60]. These simulations are usually conducted using analytic potential energy functions of the molecular mechanics type, written as a sum of an intramolecular potential for the projectile gas (in case of polyatomics), an intramolecular potential for the SAM surface, and a gas/surface intermolecular potential. The gas/surface interaction term is frequently described by a sum of two-body functions based on the Buckingham potential [61], which seems to be more realistic than the Lennard-Jones potential [62] from a physical point of view [63]. The latter, however, is commonly employed in molecular dynamics simulations due to its advantage in terms of CPU-time consumption. The parameters of these potential functions have been derived from fits to intermolecular potential energy curves (IPECs)

obtained by high-level ab initio calculations for interaction between the gas and a model compound representing the SAM surface.

In previous studies, parameterizations of gas/F-SAM interaction potentials were carried out using the CF_4 molecule as a model of F-SAM surfaces [48,64-66]. A similar approach was followed for the development of interaction potentials of gases with self-assembled monolayers of alkanes (H-SAM), where CH_4 was utilized as a model of the surface [37,41,44,47,49,55,58,66-68]. These simplifications are made under the assumptions that the electron densities around the C and F(H) atoms in CF_4(CH_4) are similar to those in the fluorocarbon chains of F-SAM (alkane chains of H-SAM), and that non-additive effects, associated mainly with polarization interactions, are negligible. Calculations of quantum theory of atoms in molecules [69,70] predict a slight but significant variation of the atomic properties (e.g., partial charges) of the C and F or H atoms when going from CF_4 or CH_4 to long-chain perfluoroalkanes [71,72] or long-chain alkanes [73-75]. However, Troya and co-workers have shown that parameters of pair potentials derived from calculations on the Ar/CF_4 and Ar/CH_4 systems are transferable to Ar/C_2F_6 and Ar/C_2H_4 [68], thus suggesting that the differences between the electron densities in CF_4 and CH_4 with respect to those in long chains are not significant as far as interaction potentials are concerned. Also, parameterizations performed on the NH_4^+/CH_4 and $CH_3NH_3^+$/CH_4 systems led to essentially the same intermolecular potentials in the sense that NH_4^+ and the -NH_3^+ group of $CH_3NH_3^+$ behave the same way [67].

In the first step of a typical parameterization, ab-initio IPECs are calculated for different orientations of the gas and CF_4 molecules, usually employing the supermolecule approach with frozen intramolecular geometries and correcting the energy for the basis set superposition error (BSSE) by the counterpoise method [76,77].

If the size of the projectile species is small, the molecular structure calculations may be performed using coupled cluster theory with singles, doubles, and perturbative triples excitations [CCSD(T)] [78], together with one of the various schemes reported in the literature for extrapolating the total energy to the complete (one-electron) basis-set (CBS) limit [79-88]. However, as the size of the system increases, less expensive computational methods may be required as, for example, the focal point approach of Allen and co-workers [89-91]. With this approach, highly accurate energies obtained by second-order Møller-Plesset theory (MP2) [92,93] may be combined with coupled cluster energies to give approximations to CCSD(T)/CBS energies. For large systems, even this level of calculation may be computationally prohibitive, and the practical alternatives may be reduced to one of the new generation of density functional theory (DFT) methods [94] that have been adapted to describe long-range dispersion interactions (e.g., see Ref. [95]). In this case, however, it may be highly recommended to test the performance of the selected DFT method on the system under study or on related systems.

The main objective of the work reported in this paper was to develop accurate intermolecular potentials for interactions of $SiNCS^+$ and $(CH_3)_2SiNCS^+$ ions with F-SAM surfaces. An additional aim of our study was to assess the reliability of using CF_4 as a model of an F-SAM surface for parameterizations of intermolecular potentials. For these purposes, we performed molecular structure calculations to evaluate IPECs for different orientations of the silyl ion with respect to a CF_4 molecule and, separately, to a model of F-SAM composed by nine chains of perfluorobutane, which has a large enough size to ensure its validity. Pairwise potentials of the Buckingham and Lennard-Jones types were subsequently parameterized as described in section 2.2.

2. Computational details

2.1. Molecular structure methods

Except otherwise stated, all the molecular structure calculations were performed with the TURBOMOLE 5.10 program [96]. For the smallest system investigated here, $SiNCS^+/CF_4$, a series of scan calculations were performed for the relative orientations shown graphically in Fig. 1. Cartesian coordinates for a representative point of each orientation are given in the supplementary data. Two levels of theory were employed to compute the IPECs. One was the aforementioned focal point approach [89-91]. Specifically, we first carried out a series of MP2 calculations using the resolution of the identity (RI) approximation [97,98] and the correlation-consistent basis sets aug-cc-pV*X*Z, where *X* = D, T, and Q [99], together with the corresponding auxiliary basis sets derived by Weigend et al. [100]. The following scheme of Peterson and co-workers [88] was utilized to extrapolate to the CBS limit:

$$E(n) = E_{CBS} + A e^{-(n+1)} + B e^{-(n+1)^2} \quad (1)$$

where n = 2, 3, and 4 for the MP2 energies obtained with the DZ, TZ, and QZ basis sets, respectively. Then, CCSD(T)/CBS estimates were determined with the focal-point energy relationship:

$$\text{fp-CCSD(T)/CBS} = \text{MP2/CBS} + [\text{CCSD(T)/DZ} - \text{MP2/DZ}] \quad (2)$$

where fp stands for focal point and DZ refers to the aug-cc-pVDZ basis set. The interaction energies calculated with this approach were corrected for the BSSE using the counterpoise method [76,77].

The second level of theory involved one of the DFT methods that include empirical, pairwise atomic dispersion corrections of the form $-C_6 r^{-6}$. Specifically, we

used the B97-D method of Grimme [101,102] with the RI approximation [103] and with the TZVPP (orbital and auxiliary) basis sets included in the TURBOMOLE basis set library [96]. The interaction energies calculated at this level of theory were not corrected for the BSSE, thus following the recommendations reported in the literature [101,102,104].

As shown later in the paper, the IPECs calculated by B97-D were found to be in reasonably good agreement with the fp-CCSD(T) interaction curves. For this reason, only the DFT-D method was applied to the remaining model systems considered in this work. These are $(CH_3)_2SiNCS^+/CF_4$ as well as $SiNCS^+$ and $(CH_3)_2SiNCS^+$ interacting (separately) with a model of F-SAM formed by nine chains of perfluorobutane, which, for the sake of simplicity and convenience, will be referred to as miniSAM. The orientations selected to calculate IPECs for $(CH_3)_2SiNCS^+/CF_4$ are detailed in Fig. 2, while those considered for interaction curves of $SiNCS^+$ and $(CH_3)_2SiNCS^+$ with the miniSAM are depicted in Figs. 3 and 4, respectively. The scan axis was considered to be perpendicular to the miniSAM, except for orientation H in Figs. 3 and 4. In all the molecular structure calculations, the geometries of the $SiNCS^+$, $(CH_3)_2SiNCS^+$, and CF_4 molecules were constrained to their B97-D equilibrium values. For the geometry of the miniSAM, we used the equilibrium bond lengths and bond angles of a force field of perfluoroalkanes [105], and the tilt angle and inter-chain separation determined from an optimization of an F-SAM, using the Venus 2005 program [106,107] and a force field described in detail elsewhere [48,105].

2.2. Analytical potentials and parameterization scheme

Two analytical potentials were considered in this paper to model the interaction between the silyl ion and CF_4 or the miniSAM. The first one is written as a sum of two-body Buckingham potentials [61] plus an additional term, which was necessary to include in order to increase the flexibility of the function:

$$V = \sum_i \sum_j \left\{ A e^{-B r_{ij}} - \frac{C}{r_{ij}^D} - \frac{E}{r_{ij}^F} \right\} \quad (3)$$

where the subscripts *i* and *j* refer to atoms of different interacting species. Parameters *A* to *F* were obtained by fits of the B97-D IPECs to this equation. Parameters *D* and *F* were treated as real numbers rather than as integers. The fits were conducted with the help of a genetic algorithm fully described in the literature [108]. Two different parameterizations were done. One, referred to as fit 1, was controlled by imposing the following constraints: $C \geq 0$, $E \geq 0$, $3 \leq D \leq 5$, and $5 \leq F \leq 7$. The constraints on *D* and *F* were established in order to avoid values that are too far from typical exponents for long-range interaction terms. The other parameterization, named fit 2, was guided without constraining the parameter limits. As shown later in this paper, the latter parameterization criterion leads to a set of parameters that are not transferable to the $SiNCS^+$/miniSAM system, and therefore that cannot model $SiNCS^+$/F-SAM interactions accurately.

The second potential function employed here to model the $SiNCS^+/CF_4$ interactions consists of a sum of Lennard-Jones type potentials and electrostatic terms, that is, the common representation of nonbonded interactions in most force fields employed in molecular dynamics simulations:

$$V = \sum_i \sum_j \left\{ \frac{A}{r_{ij}^B} - \frac{C}{r_{ij}^D} + \frac{q_i q_j}{r_{ij}} \right\} \quad (4)$$

where parameters A and C are positive and q_i and q_j are the partial charges of atoms i and j obtained by B97-D/TZVPP calculations using the Merz-Singh-Kolman scheme [109,110], which produces charges fitted to the electrostatic potential. These calculations were performed with the Gaussian 03 package [111]. To increase the flexibility of the function, parameter B was allowed to vary between 8.0 and 13.0, and D between 5.0 and 7.0. As discussed in the next section, the potential function of Eq. 4 did not give a good representation of the intermolecular interactions in $SiNCS^+/CF_4$. Consequently, for the remaining systems investigated here, that is, $(CH_3)_2SiNCS^+/CF_4$, $SiNCS^+$/miniSAM, and $(CH_3)_2SiNCS^+$/miniSAM, we used Eq. 3 with the parameter constraints indicated above (i.e., fit 1). For the systems involving the miniSAM model, orientation H was not used for the parameterization but for a test of the reliability of the parameterized potential function. In addition, and in order to improve the fittings, two different types of C and F atoms in the perfluorobutane chains were considered and denoted by C_3 and F_3 (perfluoromethyl atoms), and C_2 and F_2 (perfluoromethylene atoms).

3. Results and discussion

3.1. Molecular structure calculations

The IPECs calculated for the $SiNCS^+/CF_4$ system at the B97-D/TZVPP level of theory are compared in Fig. 5 with those obtained by fp-CCSD(T) computations as described previously. The inset graphs, displaying the attractive wells in an expanded scale, show well depths in the range 0.8-2.8 kcal/mol. Values of the well depths for all

the orientations and systems investigated here are collected in the supplementary information. The most favorable orientation for attractive interaction is G, for which the fp-CCSD(T) and B97-D calculations give well depths of 2.4 and 2.8 kcal/mol, respectively, at $R_{N\text{-}C}$ distances around 3.6 Å. In this orientation, the silyl ion approaches a face of CF_4 perpendicularly to the scan axis and with the N atom in line with the C-F bond that is parallel to that axis.

The differences between the IPECs obtained by the B97-D and the fp-CCSD(T) calculations are only apparent in the inset graphs. In general, the B97-D potential energy curves are slightly more attractive than those obtained by the fp-CCSD(T) calculations. The largest discrepancies (in absolute values) in the well depths occur for orientations G and C (0.4 kcal/mol in both cases); the latter corresponds to $SiNCS^+$ approaching perpendicularly to one face of the CF_4 molecule and with Si as the attacking atom. On average, the relative deviation between the fp-CCSD(T) and the B97-D well depths is 17.8%. For the repulsive part, we calculated average relative deviations of 6.2% and 8.9% for the energy ranges 10-100 and 100-1500 kcal/mol, respectively. Although these deviations are significant, the quality of the B97-D IPECs, as compared with the fp-CCSD(T) curves, is satisfactory, at least from a semiquantitative point of view. Also, as shown later, the errors in the fittings, in the best cases, are rather close to these values. For these reasons, we only employed the B97-D method for the $(CH_3)_2SiNCS^+/CF_4$ system, as well as for the systems involving the miniSAM model and for the parameterizations of the analytical potentials.

Figure 6 depicts the B97-D potential energy curves for $(CH_3)_2SiNCS^+$ interacting with CF_4 in the 12 different orientations described in Fig. 2. The most attractive interaction occurs for orientation G; this is one of the orientations in which $(CH_3)_2SiNCS^+$ approaches the CF_4 molecule with its symmetry axis perpendicularly to

the scan axis. The well depth of the corresponding IPEC is 4.0 kcal/mol and the minimum is located at a N-C separation of ca. 3.5 Å. Similarly, the IPECs of orientations C and D have well depths close to 4 kcal/mol. The IPECs of orientations A and B are very similar to those of the corresponding orientations (i.e., A and B) in the $SiNCS^+/CF_4$ system. This result could be anticipated because methyl groups are, in general, rather weak electron donors, and because in both orientations the silyl ion approaches the CF_4 molecule with its symmetry axis collinearly to one C-F bond and with the sulfur as the attacking atom.

The IPECs obtained by the B97-D/TZVPP calculations for the $SiNCS^+$ and $(CH_3)_2SiNCS^+$ ions interacting with the miniSAM are shown in Figs. 7 and 8, respectively. The intermolecular distance employed to picture the IPECs in most plots (A-G, see also Figs. 3 and 4) is defined as the distance between a selected atom of the silyl ion and the plane formed by the closest F-atom layer of the miniSAM. The selected atom is the one which is closest to the miniSAM, excluding hydrogen atoms in the case of $(CH_3)_2SiNCS^+$. For orientations in which the molecular axis of the silyl ion is perpendicular to the scan axis, all the atoms (except hydrogens) are at the same distance from the miniSAM. Negative values of *R* indicate penetration into the miniSAM. The distances used to depict the IPECs for orientation H in Figs. 7 and 8 do not follow the above definition. In Fig. 7, we considered the distance between the carbon atom of the silyl ion and the first carbon atom of the central chain of the miniSAM (see Fig. 3), and in Fig. 8 we used the distance between Si and the second C atom of the central chain (see Fig. 4). As indicated before, we used the IPECs of orientation H for tests to assess the quality of the potentials but not for the fittings. For several orientations, the IPECs undulate in the region corresponding to negative values of *R*, which is associated with partial or even complete penetration of the silyl ion into the miniSAM structure. This

type of behavior takes place especially in the $SiNCS^+$/miniSAM system because the shape of the ion facilitates the entrance into the miniSAM. For $(CH_3)_2SiNCS^+$, this feature occurs only for orientation *D*, in which the symmetry axis of the ion is collinear to the direction of attack and the sulfur atom approaches the surface first, so that partial penetration of the silyl ion into the surface is facilitated.

The well depths of the IPECs calculated at the B97-D/TZVPP level for the $SiNCS^+$/miniSAM system are in the range 2.8-8.8 kcal/mol. The highest depth (8.8 kcal/mol) is found for the test orientation H and occurs at a distance $R_{C\text{-}C}$ of 6.6 Å. The IPEC of orientation C has also a substantial depth (7.9 kcal/mol at R = 1.4 Å). This orientation corresponds to $SiNCS^+$ directed toward a hole of the miniSAM, with the molecular axis collinear to the scan axis, and with Si as the attacking atom. Orientation D is similar, but the ion attacks the surface with the sulfur atom. The corresponding well depth is 4.6 kcal/mol (at R = 1.8 Å). Orientations E, F, and G, in which the ion approaches the surface with the molecular axis perpendicularly to the surface normal, have IPECs with depths in the range 6.6-6.9 kcal/mol and located at distances around 2.8 Å.

For $(CH_3)_2SiNCS^+$ interacting with the miniSAM, the B97-D calculations predict IPECs with well depths ranging from 2.2 kcal/mol, for orientation B, to 9.9 kcal/mol, for orientation E. Orientation G has also an IPEC with a significant depth (9.6 kcal/mol). Both orientations E and G involve configurations in which the ion approaches the surface with its symmetry axis perpendicular to the surface normal. According to the values of the calculated well depths (given in the supplementary information) it appears that the interaction between $(CH_3)_2SiNCS^+$ and the miniSAM in the attractive region is slightly stronger than that between $SiNCS^+$ and the miniSAM. This is qualitatively in line with the conclusion of Cooks and co-workers [1,5],

mentioned in the Introduction, that inclusion of methyl groups increases the attractive intermolecular interaction with the monolayer. However, the differences in the strengths of the interactions of these two silyl ions with the miniSAM do not seem to be sufficiently marked to justify their different behavior for soft-landing observed experimentally.

3.2. Analytical potentials

The IPECs of the $SiNCS^+/CF_4$ system calculated at the B97-D/TZVPP level of theory were fitted to Eqs. 3 and 4. The fits are shown graphically in Fig. 9, in which the DFT data are represented as open circles. The solid lines in red correspond to the IPECs obtained with Eq. 3 and the parameters derived from fit 1, which are collected in Table 1. The lines in cyan were computed with the parameters derived from fit 2, which are listed in Table 2. The black lines are the interaction curves obtained from the fit to Eq. 4; the corresponding parameters are listed in Table 3 and the partial charges calculated with the Merz-Singh-Kolman approach [109,110] are shown in Fig. 10. Errors associated with the fits are tabulated in the supplementary data. They were calculated as average values of energy deviations for the energy ranges of 10-100 and 100-1500 kcal/mol, and for the well depths. The most remarkable result is that the latter potential energy function, that is, the combination of a Lennard-Jones type potential and an electrostatic term, is unable to accurately model the whole range of interaction energies investigated in this study. Specifically, the average errors for the well depths and for the energy ranges 10-100 and 100-1500 kcal/mol are 58.4%, 92.1%, and 58.6%, respectively. For fit 1, the average errors for the well depths and for the energy range 10-100 kcal/mol are about 9%, and that for the energy range 100-1500 kcal/mol is

6.2%. As seen in Table 3, the values of the parameters obtained for Eq. 4 correspond to limit values imposed in the parameterization procedure. Specifically, all *B* values are equal to 8, the lower limit considered in this work; all *C* values are zero, except for the N-C and C-C pair potentials but the associated *D* values are 5, which is the lower limit set for this exponent. This result suggests that there is an intrinsic limitation in the applicability of Eq. 4 to the systems investigated here. The performance of this type of potentials could be improved if an electrostatic damping factor is introduced to correct the unphysical behavior of the electrostatic term at short distances [112]. We notice that electrostatic damping factors are not used in most force fields implemented in molecular dynamics programs because the conditions employed in typical simulations do not lead to configurations of high energy repulsions. In fact, the usual force fields are parameterized to represent as accurately as possible the attractive regions only. Because potentials written in the form of Eq. 3 give good agreement with the B97-D IPECs, as shown in Fig. 9, we decided to use them here rather than using potentials based on Eq. 4. It is interesting to note that the fit to Eq. 3 performed under the constraints detailed in section 2.2 (i.e., fit 1) is practically as good as that conducted without constraints. The errors for fit 2 are only slightly (≈2%) smaller than those of fit 1. Also worth noting is the result that the fit made without constraints led to some parameters whose values are far from typical ranges of exponents in analytical functions representing intermolecular interactions. The most acute example is the value of 19.791 obtained for the *D* parameter corresponding to the S-F pair potential.

One of the objectives of this study was to test whether CF_4 can be used as a good model of an F-SAM surface for parameterization purposes. To this end, we calculated IPECs for the eight orientations of the $SiNCS^+$/miniSAM interacting system, using the analytical function given by Eq. 3 and the parameters listed in Tables 1 and 2, and we

compared them with the IPECs predicted with the B97-D method, shown as open circles in Fig. 7. Two remarkable results are apparent from this comparison. First, the parameters obtained from fit 1 (Table 1) are transferable to the $SiNCS^+$/miniSAM system, since the IPECs calculated with them (red lines in Fig. 7) agree reasonably well with the B97-D curves; the largest deviations (25.5%), obtained for the energy range 10-100 kcal/mol, are acceptable for qualitative or semiquantitative purposes. And second, the IPECs calculated with the parameters obtained from fit 2 in the $SiNCS^+/CF_4$ system (cyan lines) show significant disagreement with the B97-D curves. In particular, the average deviation for the well depths amounts 62.5%, whereas that for fit 1 is 8.4%. Therefore, for parameterization purposes, CF_4 may be used as a model of F-SAM, provided some care is taken in the parameterization conditions. For completeness, we fitted the B97-D curves calculated for the $SiNCS^+$/miniSAM system to Eq. 3, using the same constraints imposed in fit 1 for $SiNCS^+/CF_4$. The fit led to the set of parameters listed in Table 4 and the black lines depicted in Fig. 7. For this fit, the largest average deviation (12.2%) was obtained for the energy range 10-100 kcal/mol. It can be seen that the IPECs computed with this potential agree quite well with those obtained with the set of parameters of Table 1 (red lines), derived using the $SiNCS^+/CF_4$ system. The most significant deviations appear in regions, at negative values of *R*, where undulations are exhibited.

For the $(CH_3)_2SiNCS^+/CF_4$ system, the fit of the B97-D data to Eq. 3 is shown graphically in Fig. 6 and the parameters are listed in Table 5. As can be seen, for all the orientations described in Fig. 2, the analytical potential gives IPECs (red lines) in good agreement with the B97-D curves (open circles). The largest average error of the fit is 14.3%, and corresponds to the energy range 10-100 kcal/mol. Using the parameters of Table 5, we calculated IPECs for $(CH_3)_2SiNCS^+$ interacting with the miniSAM for all

the orientations of Fig. 4, and we compared them, in Fig. 8, with the IPECs determined at the B97-D level of theory. We also performed a fit of the B97-D curves of the $(CH_3)_2SiNCS^+$/miniSAM system to Eq. 3 (orientation H was not used in the fitting), which led to the black lines in Fig. 8 and the parameters reported in Table 6. From the comparison, it is clear that the analytical potential derived from the $(CH_3)_2SiNCS^+/CF_4$ fit is in rather good agreement with that obtained from the $(CH_3)_2SiNCS^+$/miniSAM fit, and both potentials reproduce the B97-D IPECs of the $(CH_3)_2SiNCS^+$/miniSAM system reasonably well. The largest differences between the well depths computed with Eq. 3 and the parameters of Table 5 and those calculated at the B97-D level are less than 2 kcal/mol, and correspond to orientations E, F, and G. These results, therefore, corroborate that CF_4 may be a valid model for developing intermolecular potentials for interactions of gases with F-SAM surfaces.

4. Conclusions

Molecular structure calculations were performed to compute intermolecular potential energy curves for interaction of $SiNCS^+$ and $(CH_3)_2SiNCS^+$ ions with CF_4 and with nine chains of perfluorobutane, which constitute a reliable model of an F-SAM surface for parameterizing intermolecular potentials. For the $SiNCS^+/CF_4$ system, the B97-D/TZVPP level of theory gives IPECs in reasonable agreement with fp-CCSD(T)/CBS calculations, which validates the use of the DFT-D method for the purposes of the present investigation.

The comparison between the B97-D IPECs calculated for the $SiNCS^+$/miniSAM system and those computed for $(CH_3)_2SiNCS^+$/miniSAM shows, as expected, that inclusion of the methyl groups results, on average, in a slightly more attractive

interaction in the well region. However, because the differences in the interaction strengths are rather small, there may be other factors that account for the contrasting behavior of these two ions for soft-landing onto F-SAM surfaces. For example, (i) entrapment of $(CH_3)_2SiNCS^+$ ions due to the methyl groups, as suggested by Cooks and co-workers [1,5]; (ii) additional degrees of freedom for $(CH_3)_2SiNCS^+$ (in particular the two rotors) may result in it receiving more internal energy and thus decreasing the amount in the projectile's translation as it scatters off the surface, which will increase the soft-landing efficiency; (iii) a much higher probability of ion neutralization for $SiNCS^+$, provided the ions can easily penetrate into the monolayer and approach the gold surface. All these possible factors will be investigated in future work.

Intermolecular pairwise potentials were parameterized by fits to the B97-D IPECs. The present study shows that, for the whole range of energies investigated, the B97-D IPECs calculated for interactions of silyl ions with CF_4 and the miniSAM cannot be accurately fitted to a combination of a Lennard-Jones type of potential and an electrostatic term for point charges. The analytical potentials given by Eq. 3 and the parameters obtained from the fits performed on the $SiNCS^+/CF_4$ and $(CH_3)_2SiNCS^+/CF_4$ systems can reproduce the B97-D IPECs calculated for the interaction of the silyl ions with the miniSAM. This supports the use of CF_4 as a simple, yet valid model of F-SAM for developing intermolecular potentials for interactions of gases with F-SAM surfaces. The intermolecular potentials derived here will be used, in future work, for exploring the dynamics of collisions and soft-landing of these silyl ions with a self-assembled monolayer surface of perfluorinated alkanethiols. Finally, we emphasize that, due to the complexity of this kind of systems, the use of fitting tools based on genetic algorithms are extremely valuable to obtain a good set of potential parameters.

Acknowledgements

J.J.N., E.M.-N. and S.V.R. thank the "Ministerio de Educación y Ciencia" (Grant No. CTQ2006-06301) and "Xunta de Galicia" (Grant No. PGDIT07PXIB209072PR and "Axuda para Consolidación e Estruturación de unidades de investigación competitivas do Sistema Universitario de Galicia, Xunta de Galicia 2007/050, cofinanciada polo FEDER 2007-2013") for financial support. The contribution by W. L. Hase was supported by the National Science Foundation Partnership in International Research and Education (PIRE) Grant No. OISE-0730114 and the Robert A. Welch Foundation under Grant No. D-0005. The authors thank "Centro de Supercomputación de Galicia (CESGA)" for the use of its computational resources.

References

[1] S.A. Miller, H. Luo, S.J. Pachuta, R.G. Cooks, Science 275 (1997) 1447.
[2] J. Laskin, P. Wang, O. Hadjar, Phys. Chem. Chem. Phys. 10 (2008) 1079.
[3] B. Gologan, J.R. Green, J. Alvarez, J. Laskin, R. Graham Cooks, Phys. Chem. Chem. Phys. 7 (2005) 1490.
[4] B. Gologan, J.M. Wiseman, R.G. Cooks, In: Laskin J, Lifshitz C (ed) Ion soft landing: instrumentation, phenomena, and applications, John Wiley & Sons., Inc., Hoboken, New Jersey, 2006.
[5] H. Luo, S.A. Miller, R.G. Cooks, S.J. Pachuta, Int. J. Mass. Spectrom. Ion Processes 174 (1998) 193.
[6] J. Shen, Y.H. Yim, B. Feng, V. Grill, C. Evans, R.G. Cooks, Int. J. Mass. Spectrom. 182-183 (1999) 423.
[7] M.B.J. Wijesundara, L. Hanley, B. Ni, S.B. Sinnott, Proc. Natl. Acad. Sci. U. S. A. 97 (2000) 23.
[8] M.B.J. Wijesundara, E. Fuoco, L. Hanley, Langmuir 17 (2001) 5721.
[9] M. Volny, A. Sengupta, C.B. Wilson, B.D. Swanson, E.J. Davis, F. Turecek, Anal. Chem. 79 (2007) 4543.
[10] S. Rauschenbach, R. Vogelgesang, N. Malinowski, J.r.W. Gerlach, M. Benyoucef, G. Costantini, Z. Deng, N. Thontasen, K. Kern, ACS Nano 3 (2009) 2901.
[11] Z. Nie, G. Li, M.P. Goodwin, L. Gao, J. Cyriac, R.G. Cooks, J. Am. Soc. Mass. Spectrom. 20 (2009) 949.
[12] S.A. Miller, H. Luo, X. Jiang, H.W. Rohrs, R.G. Cooks, Int. J. Mass. Spectrom. Ion Processes 160 (1997) 83.
[13] B. Kaiser, T.M. Bernhardt, B. Stegemann, J. Opitz, K. Rademann, Phys. Rev. Lett. 83 (1999) 2918.
[14] W. Yamaguchi, K. Yoshimura, Y. Tai, Y. Maruyama, K. Igarashi, S. Tanemura, J. Murakami, Chem. Phys. Lett. 311 (1999) 341.
[15] S. Messerli, S. Schintke, K. Morgenstern, A. Sanchez, U. Heiz, W.-D. Schneider, Surf. Sci. 465 (2000) 331.
[16] M. Mitsui, S. Nagaoka, T. Matsumoto, A. Nakajima, J. Chem. Phys. B 110 (2006) 2968.
[17] F. Claeyssens, S. Pratontep, C. Xirouchaki, R.E. Palmer, Nanotechnology 17 (2006) 805.
[18] S.C. Nanita, Z. Takats, R.G. Cooks, S. Myung, D.E. Clemmer, J. Am. Soc. Mass. Spectrom. 15 (2004) 1360.
[19] S. Nagaoka, K. Ikemoto, T. Matsumoto, M. Mitsui, A. Nakajima, J. Phys. Chem. C 112 (2008) 6891.
[20] S. Nagaoka, K. Ikemoto, T. Matsumoto, M. Mitsui, A. Nakajima, J. Phys. Chem. C 112 (2008) 15824.
[21] T. Matsumoto, S. Nagaoka, K. Ikemoto, M. Mitsui, M. Ara, H. Tada, A. Nakajima, Eur. Phys. J. D 52 (2009) 99.
[22] J. Laskin, P. Wang, O. Hadjar, J. Phys. Chem. C 114 (2010) 5305.
[23] G.E. Johnson, M. Lysonski, J. Laskin, Anal. Chem. 82 (2010) 5718.
[24] K. Ikemoto, S. Nagaoka, T. Matsumoto, M. Mitsui, A. Nakajima, J. Phys. Chem. C 113 (2009) 4476.
[25] B. Gologan, Z. Takáts, J. Alvarez, J.M. Wiseman, N. Talaty, Z. Ouyang, R.G. Cooks, J. Am. Soc. Mass. Spectrom. 15 (2004) 1874.
[26] J. Alvarez, R.G. Cooks, S.E. Barlow, D.J. Gaspar, J.H. Futrell, J. Laskin, Anal. Chem. 77 (2005) 3452.
[27] J. Alvarez, J.H. Futrell, J. Laskin, J. Phys. Chem. A 110 (2006) 1678.

[28] M. Volny, W.T. Elam, B.D. Ratner, F. Turecek, Anal. Chem. 77 (2005) 4846.
[29] P. Wang, J. Laskin, Angew. Chem. Int. Ed. 47 (2008) 6678.
[30] O. Hadjar, P. Wang, J.H. Futrell, J. Laskin, J. Am. Soc. Mass. Spectrom. 20 (2009) 901.
[31] Z. Ouyang, Z. Takats, T.A. Blake, B. Gologan, A.J. Guymon, J.M. Wiseman, J.C. Oliver, V.J. Davisson, R.G. Cooks, Science 301 (2003) 1351.
[32] M. Volny, W.T. Elam, A. Branca, B.D. Ratner, F. Turecek, Anal. Chem. 77 (2005) 4890.
[33] B. Feng, D.S. Wunschel, C.D. Masselon, L. Pasa-Tolic, R.D. Smith, J. Am. Chem. Soc. 121 (1999) 8961.
[34] G. Siuzdak, B. Bothner, M. Yeager, C. Brugidou, C.M. Fauquet, K. Hoey, C.-M. Change, Chem. Biol. 3 (1996) 45.
[35] C. Fenselau, P.A. Demirev, Mass Spectrom. Rev. 20 (2001) 157.
[36] J.C. Love, L.A. Estroff, J.K. Kriebel, R.G. Nuzzo, G.M. Whitesides, Chem. Rev. 105 (2005) 1103.
[37] W.A. Alexander, B.S. Day, H.J. Moore, T.R. Lee, J.R. Morris, D. Troya, J. Chem. Phys. 128 (2008) 014713.
[38] D. Troya, G.C. Schatz, J. Chem. Phys. 120 (2004) 7696.
[39] T. Yan, W.L. Hase, Phys. Chem. Chem. Phys 2 (2000) 901.
[40] T. Yan, W.L. Hase, J.R. Barker, Chem. Phys. Lett. 329 (2000) 84.
[41] T. Yan, W.L. Hase, J. Phys. Chem. B 106 (2002) 8029.
[42] T. Yan, N. Isa, K.D. Gibson, S.J. Sibener, W.L. Hase, J. Phys. Chem. A 107 (2003) 10600.
[43] T. Yan, W.L. Hase, J. Phys. Chem. A 105 (2001) 2617.
[44] B.S. Day, J.R. Morris, D. Troya, J. Chem. Phys. 122 (2005) 214712.
[45] B.S. Day, J.R. Morris, W.A. Alexander, D. Troya, J. Phys. Chem. A 110 (2006) 1319.
[46] G. Li, S.B.M. Bosio, W.L. Hase, J. Mol. Struc. 556 (2000) 43.
[47] U.S. Tasic, T. Yan, W.L. Hase, J. Phys. Chem. B 110 (2006) 11863.
[48] E. Martínez-Núñez, A. Rahaman, W.L. Hase, J. Phys. Chem. C 111 (2007) 354.
[49] O. Meroueh, W.L. Hase, Phys. Chem. Chem. Phys 3 (2001) 2306.
[50] S.A. Vázquez, J.R. Morris, A. Rahaman, O.A. Mazyar, G. Vayner, S.V. Addepalli, W.L. Hase, E. Martínez-Núñez, J. Phys. Chem. A 111 (2007) 12785.
[51] U. Tasic, D. Troya, Phys. Chem. Chem. Phys. 10 (2008) 5776.
[52] W.A. Alexander, J.R. Morris, D. Troya, J. Phys. Chem. A 113 (2009) 4155.
[53] W.A. Alexander, J.R. Morris, D. Troya, J. Chem. Phys. 130 (2009) 084702.
[54] J.P. Layfield, D. Troya, J. Chem. Phys. 132 (2010) 134307.
[55] O. Meroueh, W.L. Hase, J. Am. Chem. Soc. 124 (2002) 1524.
[56] L. Yang, O.A. Mazyar, U. Lourderaj, J. Wang, M.T. Rodgers, E. Martínez-Núñez, S.V. Addepalli, W.L. Hase, J. Phys. Chem. C 112 (2008) 9377.
[57] G.L. Barnes, W.L. Hase, J. Am. Chem. Soc. 131 (2009) 17185.
[58] S.B.M. Bosio, W.L. Hase, J. Chem. Phys. 107 (1997) 9677.
[59] J.J. Nogueira, S.A. Vázquez, O.A. Mazyar, W.L. Hase, B.G. Perkins Jr., D.J. Nesbitt, E. Martínez-Núñez, J. Phys. Chem. A 113 (2009) 3850.
[60] J.J. Nogueira, S.A. Vazquez, U. Lourderaj, W.L. Hase, E. Martinez-Nunez, J. Phys. Chem. C 114 (2010) 18455.
[61] R.A. Buckingham, Proc. R. Soc. Lond. A 168 (1938) 264.
[62] J.E. Jones, Proc. R. Soc. Lond. A 106 (1924) 463.
[63] I.G. Kaplan, Intermolecular Interactions: Physical Picture, Computational Methods and Model Potentials, JohnWiley&Sons, Ltd., Chichester, 2006.
[64] G. Vayner, Y. Alexeev, J. Wang, T.L. Windus, W.L. Hase, J. Phys. Chem. A 110 (2005) 3174.
[65] J. Wang, W.L. Hase, J. Chem. Phys. B 109 (2005) 8320.
[66] W.A. Alexander, D. Troya, J. Phys. Chem. A 110 (2006) 10834.
[67] B. Deb, W. Hu, K. Song, W.L. Hase, Phys. Chem. Chem. Phys. 10 (2008) 4565.
[68] U. Tasic, P. Hein, D. Troya, J. Phys. Chem. A 111 (2007) 3618.

[69] R.F.W. Bader, Atoms in Molecules: A Quantum Theory, Oxford University Press, Oxford, UK, 1990.
[70] R.F.W. Bader, Chem. Rev. 91 (1991) 893.
[71] P.B. Quiñónez, A. Vila, A.M. Graña, R.A. Mosquera, Chem. Phys. 287 (2003) 227.
[72] A. Vila, R.A. Mosquera, J. Phys. Chem. A 110 (2006) 11752.
[73] K.B. Wiberg, R.F.W. Bader, C.D.H. Lau, J. Am. Chem. Soc. 109 (1987) 985.
[74] R.F.W. Bader, M.T. Carroll, J.R. Cheeseman, C. Chang, J. Am. Chem. Soc. 109 (1987) 7968.
[75] L. Lorenzo, R.A. Mosquera, Chem. Phys. Lett. 356 (2002) 305.
[76] S.F. Boys, F. Bernardi, Mol. Phys. 19 (1970) 553
[77] S. Simon, M. Duran, J.J. Dannenberg, J. Chem. Phys. 105 (1996) 11024.
[78] J.A. Pople, M. Head-Gordon, K. Raghavachari, J. Chem. Phys. 87 (1987) 5968.
[79] J.M.L. Martin, Chem. Phys. Lett. 259 (1996) 669.
[80] A. Halkier, T. Helgaker, P. Jørgensen, W. Klopper, H. Koch, J. Olsen, A.K. Wilson, Chem. Phys. Lett. 286 (1998) 243.
[81] A.P. Kirk, E.W. David, Thom H. Dunning, Jr., J. Chem. Phys. 100 (1994) 7410.
[82] D.G. Truhlar, Chem. Phys. Lett. 294 (1998) 45.
[83] D.W. Schwenke, J. Chem. Phys. 122 (2005) 014107.
[84] A.J.C. Varandas, J. Chem. Phys. 126 (2007) 244105.
[85] D. Bakowies, J. Chem. Phys. 127 (2007) 164109.
[86] J.G. Hill, K.A. Peterson, G. Knizia, H.-J. Werner, J. Chem. Phys. 131 (2009) 194105.
[87] T. Helgaker, W. Klopper, D.P. Tew, Mol. Phys. 106 (2008) 2107
[88] K.A. Peterson, D.E. Woon, DunningT.H, Jr., J. Chem. Phys. 100 (1994) 7410.
[89] A.L.L. East, W.D. Allen, J. Chem. Phys. 99 (1993) 4638.
[90] B.D. Wladkowski, W.D. Allen, J.I. Brauman, J. Chem. Phys. 98 (1994) 13532.
[91] A.G. Csaszar, W.D. Allen, H.F. Schaefer III, J. Chem. Phys. 108 (1998) 9751.
[92] R.J. Bartlett, D.M. Silver, Phys. Rev. A 10 (1974) 1927.
[93] J.S. Binkley, J.A. Pople, Int. J. Quantum Chem. 9 (1975) 229.
[94] R.G. Parr, W. Yang, Density-Functional Theory of Atoms and Molecules, International Series of Monographs on Chemistry Vol. 16, Oxford University Press, New York, 1989.
[95] C.D. Sherrill, J. Chem. Phys. 132 (2010) 110902.
[96] R. Ahlrichs, M. Bär, M. Häser, H. Horn, C. Kölmel, Chem. Phys. Lett. 162 (1989) 165.
[97] O. Vahtras, J. Almlöf, M.W. Feyereisen, Chem. Phys. Lett. 213 (1993) 514.
[98] M. Feyereisen, G. Fitzgerald, A. Komornicki, Chem. Phys. Lett. 208 (1993) 359.
[99] R.A. Kendall, J.T.H. Dunning, R.J. Harrison, J. Chem. Phys. 96 (1992) 6796.
[100] F. Weigend, M. Häser, H. Patzelt, R. Ahlrichs, Chem. Phys. Lett. 294 (1998) 143.
[101] S. Grimme, J. Comp. Chem. 25 (2004) 1463.
[102] S. Grimme, J. Comp. Chem. 27 (2006) 1787.
[103] K. Eichkorn, O. Treutler, H. Ohm, M. Haser, R. Ahlrichs, Chem. Phys. Lett. 240 (1995) 283.
[104] A. Vázquez-Mayagoitia, C.D. Sherrill, E. Aprà, B.G. Sumpter, J. Chem. Theory Comput. 6 (2010) 727.
[105] O. Borodin, G.D. Smith, D. Bedrov, J. Phys. Chem. B 106 (2002) 9912.
[106] W.L. Hase, Venus 2005. Texas Tech University, 2005.
[107] X. Hu, W.L. Hase, T. Pirraglia, J. Comp. Chem. 12 (1991) 1014.
[108] J.M.C. Marques, F.V. Prudente, F.B. Pereira, M.M. Almeida, A.M. Maniero, C.E. Fellows, J. Phys. B: At. Mol. Opt. Phys. 41 (2008) 085103.
[109] B.H. Besler, K.M. Merz, P.A. Kollman, J. Comp. Chem. 11 (1990) 431.
[110] U.C. Singh, P.A. Kollman, J. Comp. Chem. 5 (1984) 129.
[111] M.J.T. Frisch, G. W.; Schlegel, H. B.; Scuseria, G. E.; Robb, M. A.; Cheeseman, J. R.; Montgomery, J. A., Jr.; Kudin, K. N.; Burant, J. C.; Millam, J. M.; Iyengar, S. S.; Tomasi, J.; Barone, V.; Mennucci, B.; Cossi, M.; Scalmani, G.; Rega, N.; Petersson, G. A.; Nakatsuji, H.; Hada, M.; Ehara, M.; Toyota, K.; Fukuda, R.; Hasegawa, J.; Ishida, M.; Nakajima, T.; Honda, Y.; Kitao, O.; Nakai, H.; Klene, M.; Li, X.; Knox, J. E.; Hratchian, H. P.; Cross, J. B.; Adamo, C.;

Jaramillo, J.; Gomperts, R.; Stratmann, R. E.; Yazyev, O.; Austin, A. J.; Cammi, R.; Pomelli, C.; Ochterski, J. W.; Ayala, P. Y.; Morokuma, K.; Voth, G. A.; Salvador, P.; Dannenberg, J. J.; Zakrzewski, G.; Dapprich, S.; Daniels, A. D.; Strain, M. C.; Farkas, O.; Malick, D. K.; Rabuck, A. D.; Raghavachari, K.; Foresman, J. B.; Ortiz, J. V.; Cui, Q.; Baboul, A. G.; Clifford, S.; Cioslowski, J.; Stefanov, B. B.; Liu, G.; Liashenko, A.; Piskorz, P.; Komaromi, I.; Martin, R. L.; Fox, D. J.; Keith, T.; Al-Laham, M. A.; Peng, C. Y.; Nanayakkara, A.; Challacombe, M.; Gill, P. M. W.; Johnson, B.; Chen, W.; Wong, M. W.; Gonzalez, C.; Pople, J. A., Gaussian 03, revision E.01. Gaussian, Inc.: Wallingford CT, 2004.

[112] G.A. Cisneros, S.N.I. Tholander, O. Parisel, T.A. Darden, D. Elking, L. Perera, J.P. Piquemal, Int. J. Quantum Chem. 108 (2008) 1905.

Table 1. Parameters of Eq. 3 obtained from fit 1 for the $SiNCS^+/CF_4$ system.[a]

	A	*B*	*C*	*D*	*E*	*F*
Si-C	6538.188	2.434	-	-	-	-
Si-F	18138.253	3.131	-196.303	4.368	-	-
N-C	101627.865	4.648	-	-	-1466.543	5.908
N-F	33037.375	3.463	-113.072	5.000	-452.264	5.546
C-C	4463.786	2.274	-	-	-671.679	7.000
C-F	6979.581	3.018	-	-	-8.469	6.012
S-C	8789.758	2.525	-8.005	5.000	-49.946	5.215
S-F	27383.103	3.308	-163.076	4.652	-115.340	5.000

[a]The units are such that the potential is in kcal/mol and distances in Å.

Table 2. Parameters of Eq. 3 obtained from fit 2 for the $SiNCS^+/CF_4$ system.[a]

	A	*B*	*C*	*D*	*E*	*F*
Si-C	11154.135	2.602	1693.381	11.737	-1767.434	8.623
Si-F	14675.277	2.966	299.087	13.523	-339.363	4.679
N-C	8259.926	4.153	2864.545	11.736	-729.107	5.456
N-F	23014.401	3.212	1055.419	5.765	-1493.217	5.302
C-C	16148.397	3.159	8807.686	4.860	-10507.434	5.179
C-F	10273.754	3.031	504.412	6.811	-688.895	5.936
S-C	184993.405	8.015	2379.662	4.972	-1783.814	6.017
S-F	33002.435	3.241	156.028	19.791	-667.150	4.782

[a]The units are such that the potential is in kcal/mol and distances in Å.

Table 3. Parameters of Eq. 4 obtained for the $SiNCS^+/CF_4$ system.[a]

	A	*B*	*C*	*D*
Si-C	1082.545	8.000	-	-
Si-F	1547.894	8.000	-	-
N-C	5560.997	8.000	-800.000	5.000
N-F	1010.489	8.000	-	-
C-C	12764.578	8.000	-1143.714	5.000
C-F	245.054	8.000	-	-
S-C	1470.957	8.000	-	-
S-F	1062.301	8.000	-	-

[a]The units are such that the potential is in kcal/mol and distances in Å.

Table 4. Parameters of Eq. 3 derived for the $SiNCS^+$/miniSAM system.[a]

	A	*B*	*C*	*D*	*E*	*F*
Si-C_3	18534.817	2.382	-564.543	4.537	-22.199	6.405
Si-C_2	64855.770	3.008	-223.620	4.486	-437.059	5.522
Si-F_3	23491.237	3.496	-126.166	4.800	-448.122	6.137
Si-F_2	23913.193	3.488	-89.798	4.581	-0.205	6.888
N-C_3	27551.371	3.687	-65.528	4.567	-956.760	5.760
N-C_2	31397.593	3.982	-313.098	4.935	-1038.343	6.187
N-F_3	35624.283	3.672	-150.146	4.953	-293.498	6.225
N-F_2	68943.696	4.558	-93.177	4.999	-229.920	6.328
C-C_3	18372.699	3.152	-37.022	4.751	-554.617	5.635
C-C_2	22315.273	3.481	-8.033	4.090	-381.924	5.992
C-F_3	5311.952	2.710	-7.966	4.574	-0.819	5.955
C-F_2	30400.976	3.348	-0.884	4.928	-600.325	5.829
S-C_3	34713.238	3.849	-125.240	4.518	-580.811	5.893
S-C_2	66403.057	4.485	-609.191	4.974	-1709.718	6.957
S-F_3	22734.176	3.083	-78.161	4.767	-238.581	5.252
S-F_2	73637.242	4.036	-2.673	4.848	-472.422	6.108

[a]The units are such that the potential is in kcal/mol and distances in Å. Subscripts 2 and 3 refer to perfluoromethylene and perfluoromethyl atoms, respectively.

Table 5. Parameters of Eq. 3 derived for the $(CH_3)_2SiNCS^+/CF_4$ system.[a]

	A	*B*	*C*	*D*	*E*	*F*
Si-C	13513.187	2.462	-3.163	4.342	-6.819	5.210
Si-F	28382.750	3.868	-45.367	3.938	-	-
N-C	162748.891	4.302	-169.184	4.801	-2022.234	5.407
N-F	35890.509	3.603	-39.288	4.936	-302.611	5.452
C-C	4331.934	2.279	-1.030	4.847	-1699.847	6.721
C-F	6942.115	2.924	-	-	-	-
S-C	7848.930	2.419	-64.457	4.837	-99.473	5.209
S-F	31990.682	3.427	-106.739	4.487	-70.368	5.002
C(Me)-C	29243.460	3.024	-1.766	3.980	-1475.676	5.856
C(Me)-F	35473.244	3.631	-42.585	4.763	-269.543	5.293
H-C	2338.852	2.891	-	-	-	-
H-F	5405.861	4.137	-	-	-	-

[a]The units are such that the potential is in kcal/mol and distances in Å.

Table 6. Parameters of Eq. 3 derived for the $(CH_3)_2SiNCS^+$/miniSAM system.[a]

	A	B	C	D	E	F
Si-C_3	17465.327	2.427	-108.231	4.686	-571.057	6.558
Si-C_2	2299.708	4.010	-117.265	4.875	-58.430	6.478
Si-F_3	32868.276	3.352	-169.112	4.614	-822.938	6.010
Si-F_2	25024.365	2.237	-4.114	4.811	-1549.042	6.793
N-C_3	27551.371	3.687	-65.528	4.567	-956.760	5.760
N-C_2	31397.593	3.982	-313.098	4.935	-1038.343	6.187
N-F_3	35624.283	3.672	-150.146	4.953	-293.498	6.225
N-F_2	68943.696	4.558	-93.177	4.999	-229.920	6.328
C-C_3	18372.699	3.152	-37.022	4.751	-554.617	5.635
C-C_2	22315.273	3.481	-8.033	4.090	-381.924	5.992
C-F_3	5311.952	2.710	-7.966	4.574	-0.819	5.955
C-F_2	30400.976	3.348	-0.884	4.928	-600.325	5.829
S-C_3	75661.708	4.015	-18.972	4.046	-446.308	5.855
S-C_2	39070.416	4.814	-172.163	4.860	-1143.539	6.634
S-F_3	33856.220	3.213	-16.978	4.748	-932.123	6.175
S-F_2	59061.975	3.906	-5.893	4.305	-368.737	6.128
C(Me)-C_3	18481.512	4.717	-79.827	4.548	-1688.458	6.224
C(Me)-C_2	75083.448	4.801	-148.959	4.987	-1021.178	5.948
C(Me)-F_3	35578.422	3.288	-20.297	4.997	-1679.091	6.451
C(Me)-F_2	48902.266	3.872	-0.801	4.070	-1681.831	6.564
H-C_3	2836.462	2.446	-7.255	4.874	-1022.163	6.637
H-C_2	16995.767	4.913	-32.338	4.483	-329.418	5.948
H-F_3	9090.716	4.573	-0.195	3.582	-5.986	5.404
H-F_2	3415.155	2.972	-6.437	4.300	-7.623	5.199

[a]The units are such that the potential is in kcal/mol and distances in Å. Subscripts 2 and 3 refer to perfluoromethylene and perfluoromethyl atoms, respectively.

Figure Captions

Figure 1. Orientations of $SiNCS^+$ and CF_4 selected for the calculation of intermolecular potential energy curves.

Figure 2. Orientations of $(CH_3)_2SiNCS^+$ and CF_4 selected for the calculation of intermolecular potential energy curves.

Figure 3. Orientations of $SiNCS^+$ and miniSAM selected for the calculation of intermolecular potential energy curves. Side and top views are shown for each orientation. The dotted lines indicate the direction of the scan axes.

Figure 4. Orientations of $(CH_3)_2SiNCS^+$ and miniSAM selected for the calculation of intermolecular potential energy curves. Side and top views are shown for each orientation. The dotted lines indicate the direction of the scan axes.

Figure 5. Comparison of the intermolecular potential energy curves of $SiNCS^+/CF_4$ calculated at the B97-D (blue circles) and fp-CCSD(T) (red circles) levels of theory. Lines are included for visual clarity.

Figure 6. Intermolecular potential energy curves of $SiNCS^+/CF_4$ calculated at the B97-D/TZVPP level (open circles) and fit to Eq. 3 (red lines).

Figure 7. Intermolecular potential energy curves of $SiNCS^+$/miniSAM calculated at the B97-D/TZVPP level, fit to Eq. 3, and comparison with the IPECs obtained with Eq. 3 and the parameters listed in Table 1 (fit 1 for $SiNCS^+/CF_4$) and Table 2 (fit 2 for $SiNCS^+/CF_4$).

Figure 8. Intermolecular potential energy curves of $(CH_3)_2SiNCS^+$/miniSAM calculated at the B97-D/TZVPP level, fit to Eq. 3, and comparison with the IPECs obtained with Eq. 3 and the parameters listed in Table 5 (fit for $(CH_3)_2SiNCS^+/CF_4$).

Figure 9. Intermolecular potential energy curves of $SiNCS^+/CF_4$ calculated at the B97-D/TZVPP level and fits to Eqs. 3 and 4. See text.

Figure 10. Partial atomic charges (in a.u.) calculated at the B97-D/TZVPP level and using the Merz-Singh-Kolman scheme.

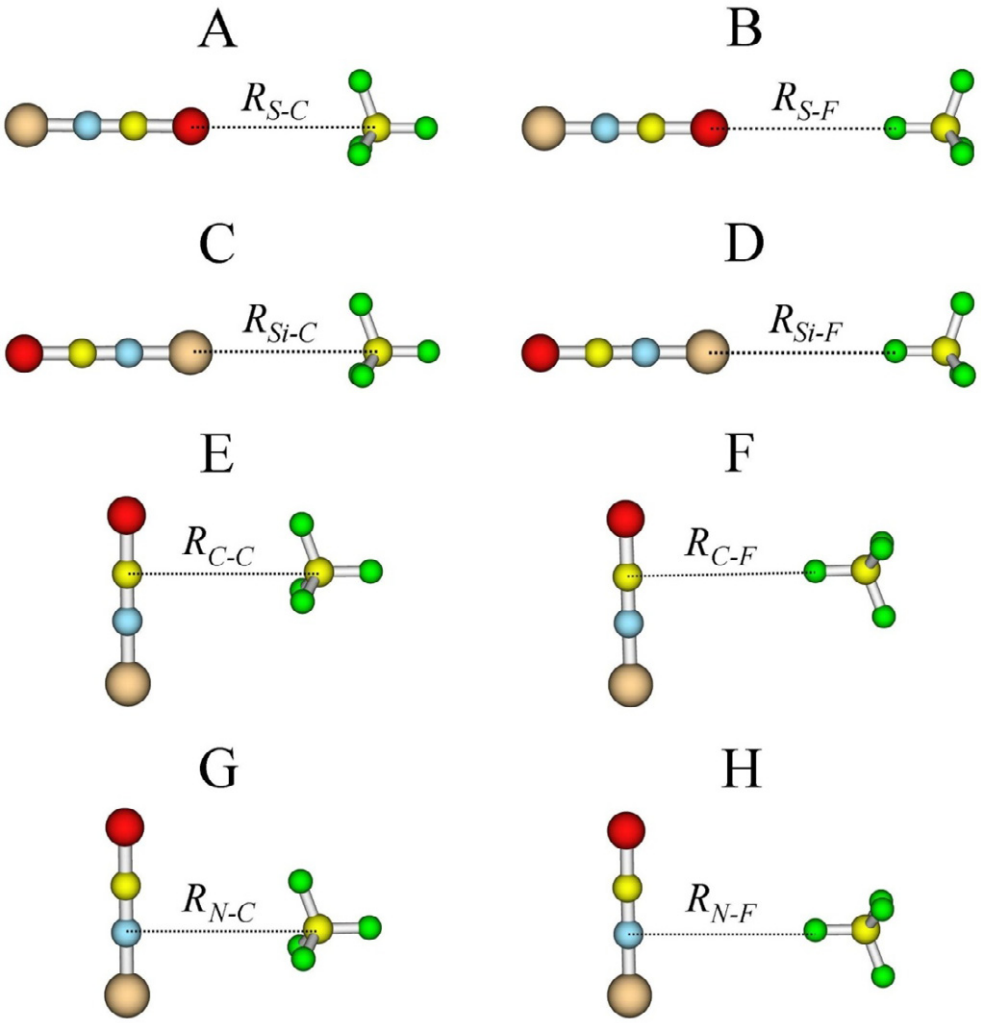

Figure 1

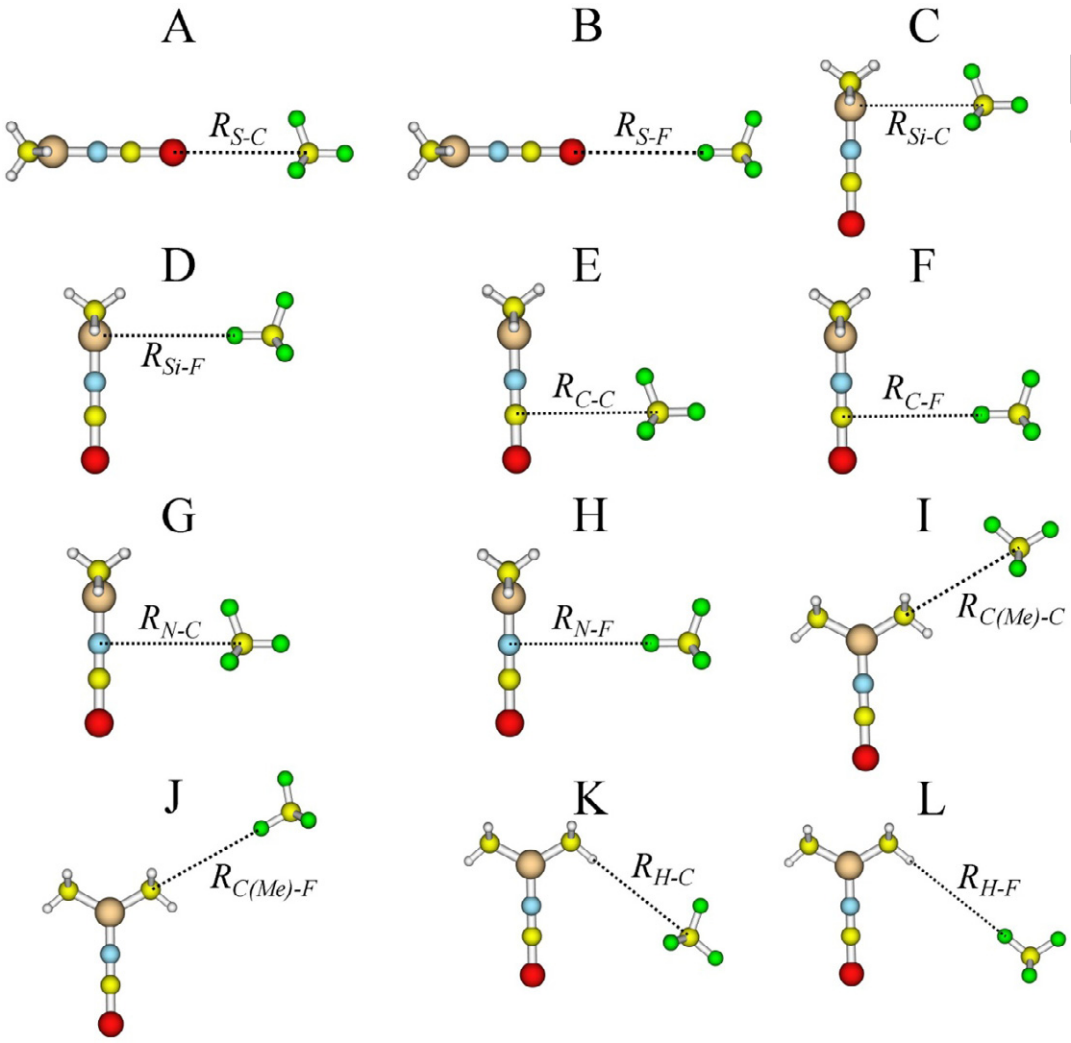
A
$R_{S\text{-}C}$
B
$R_{S\text{-}F}$
C
$R_{Si\text{-}C}$
D
$R_{Si\text{-}F}$
E
$R_{C\text{-}C}$
F
$R_{C\text{-}F}$
G
$R_{N\text{-}C}$
H
$R_{N\text{-}F}$
I
$R_{C(Me)\text{-}C}$
J
$R_{C(Me)\text{-}F}$
K
$R_{H\text{-}C}$
L
$R_{H\text{-}F}$

Figure 2

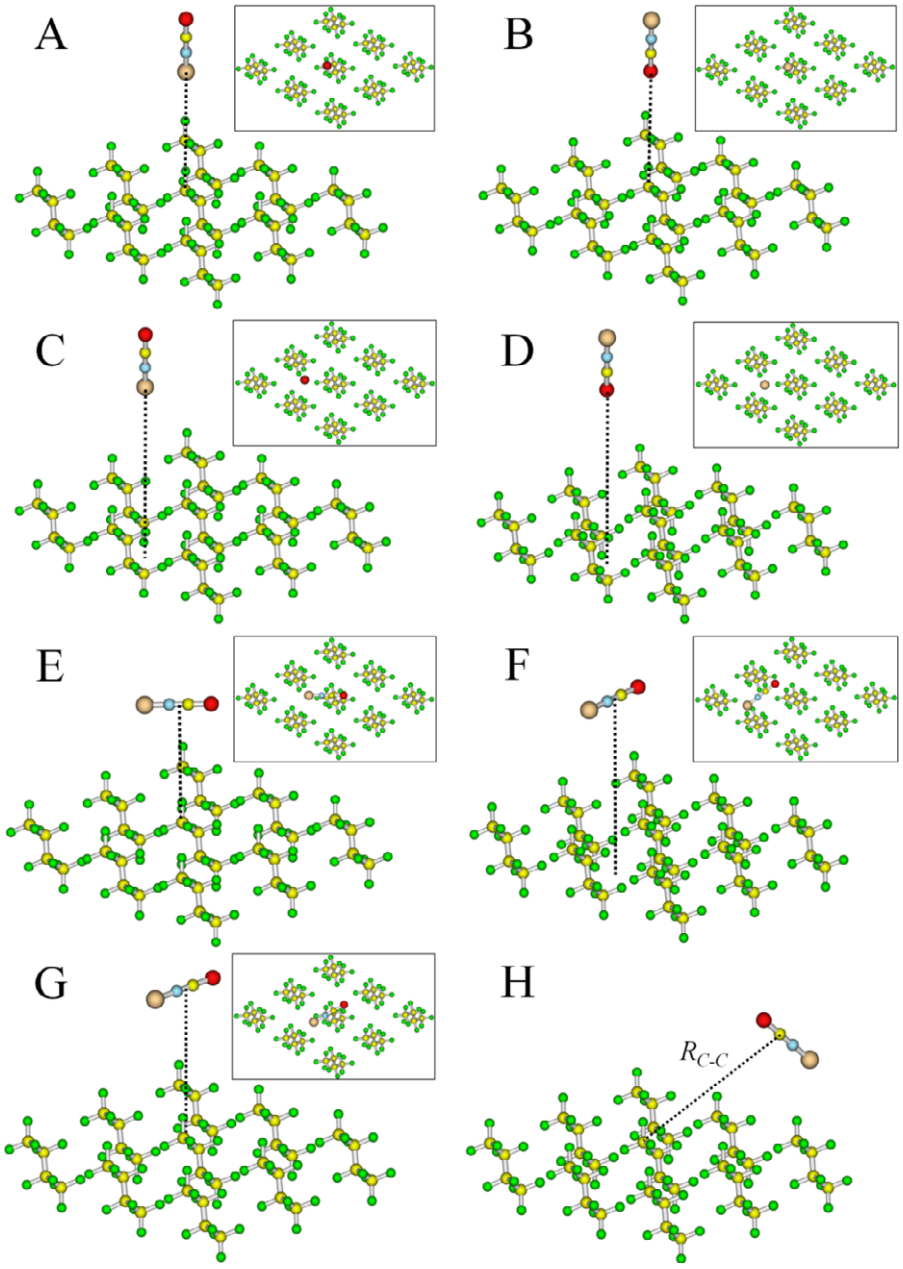

Figure 3

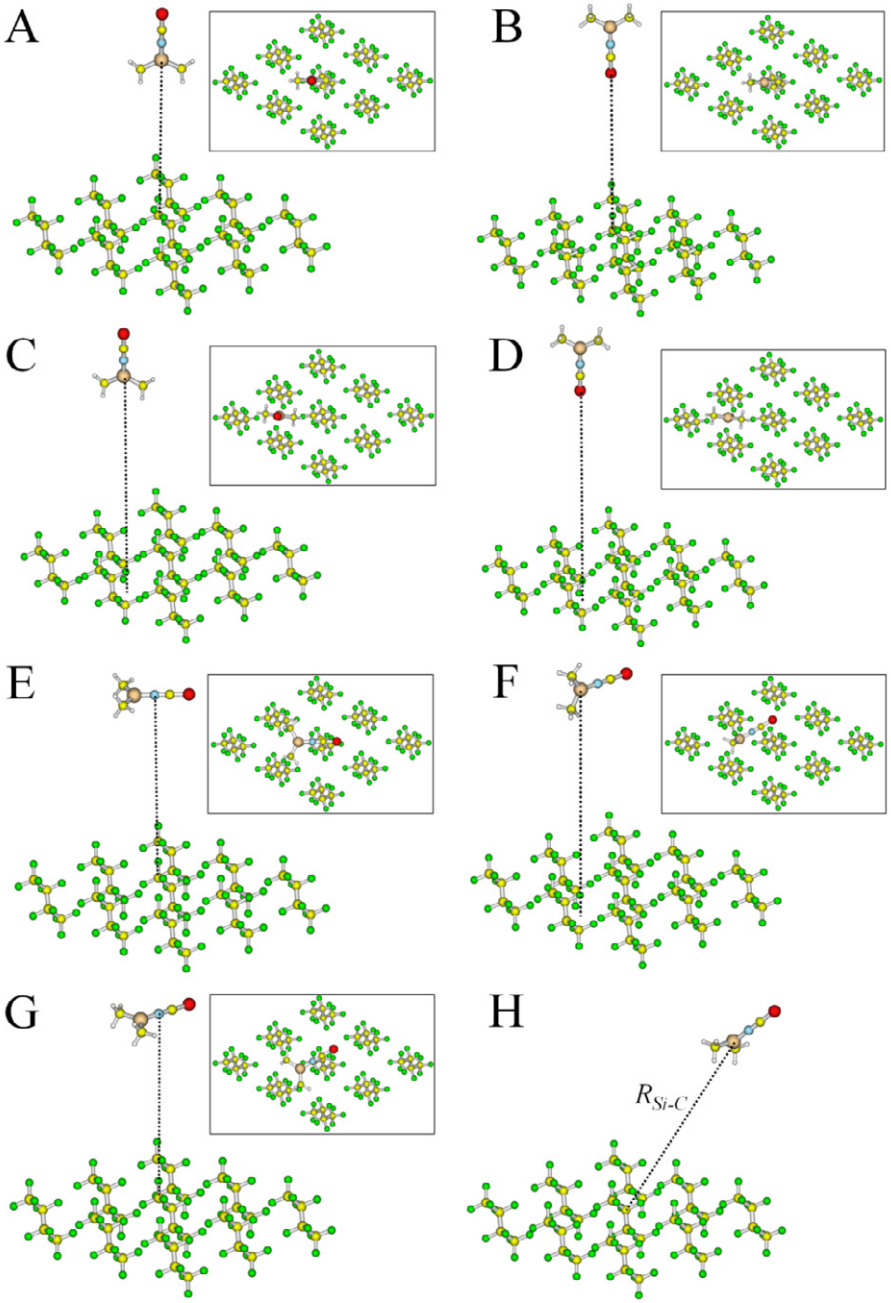

Figure 4

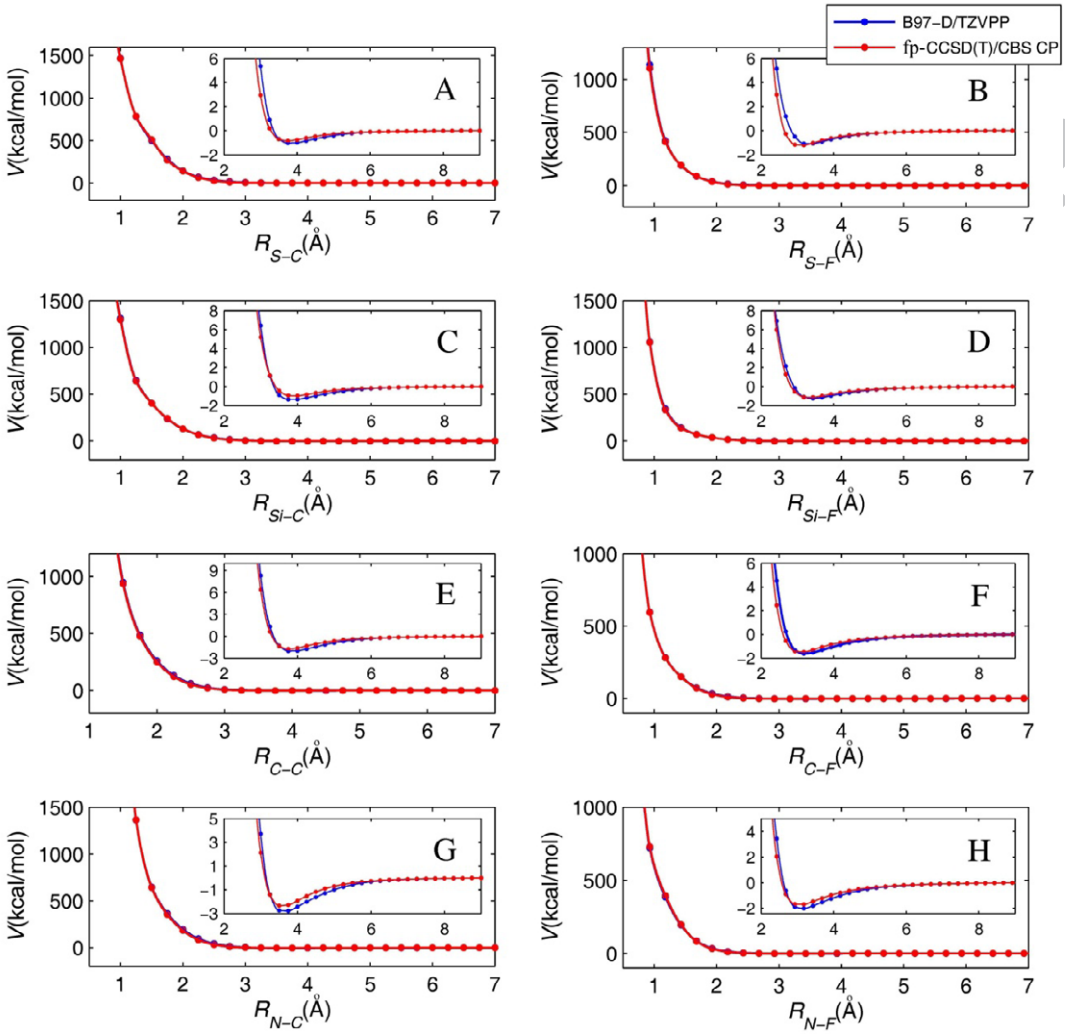

Figure 5

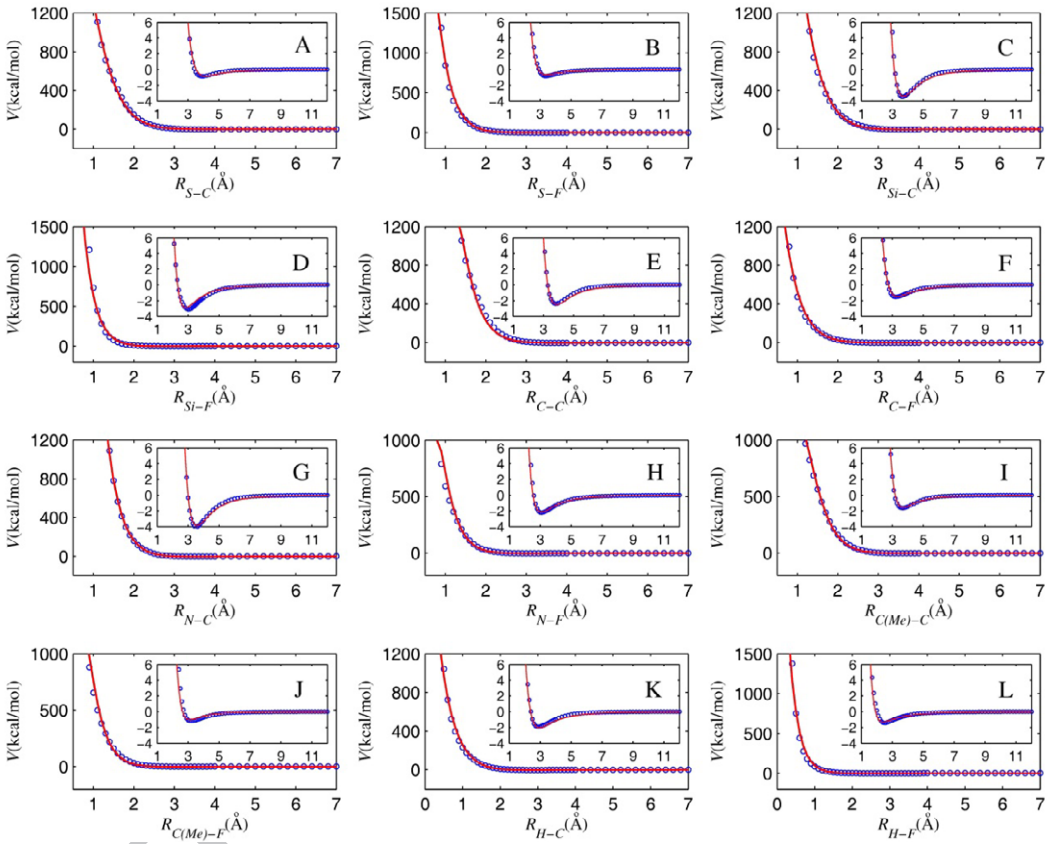

Figure 6

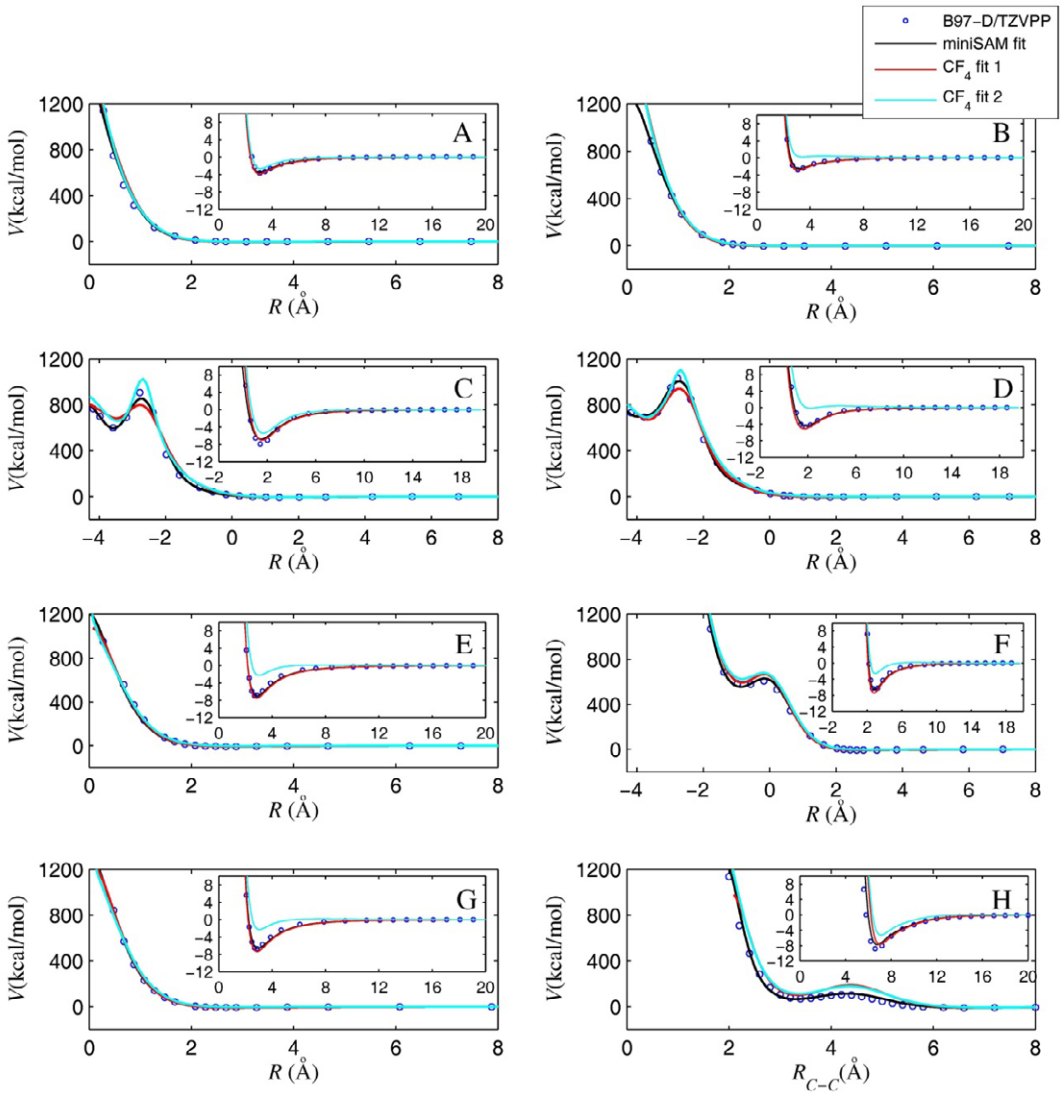

Figure 7

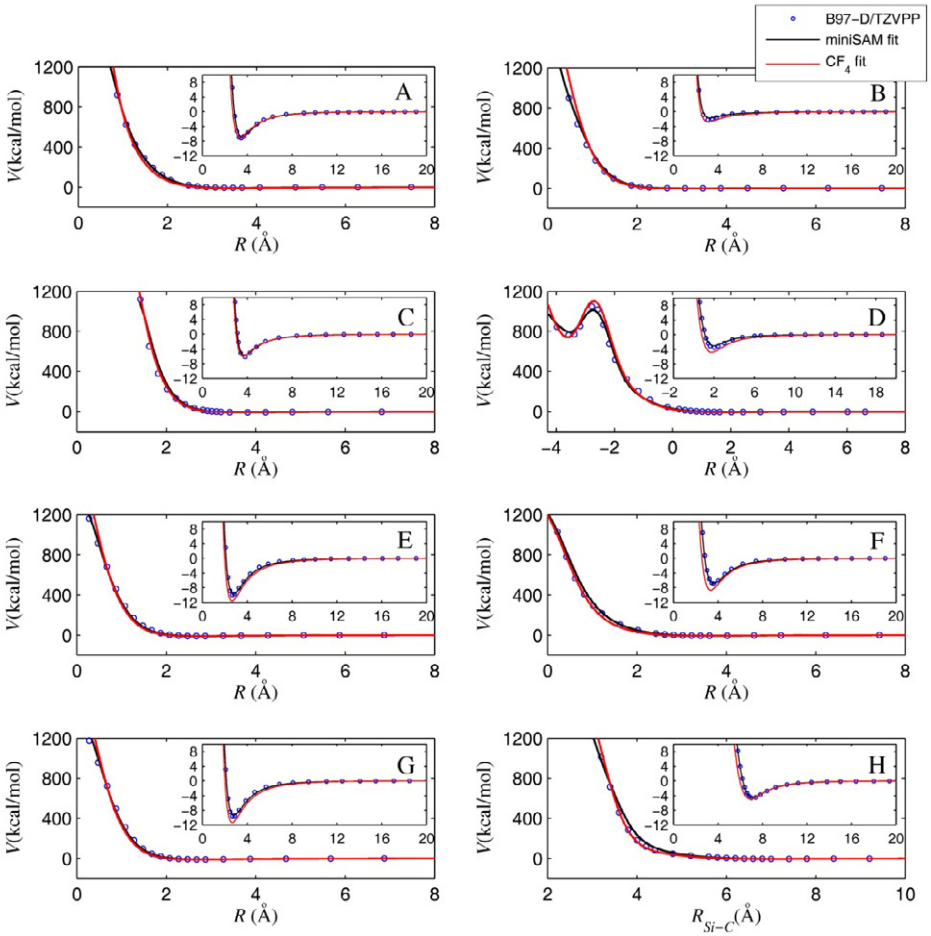

Figure 8

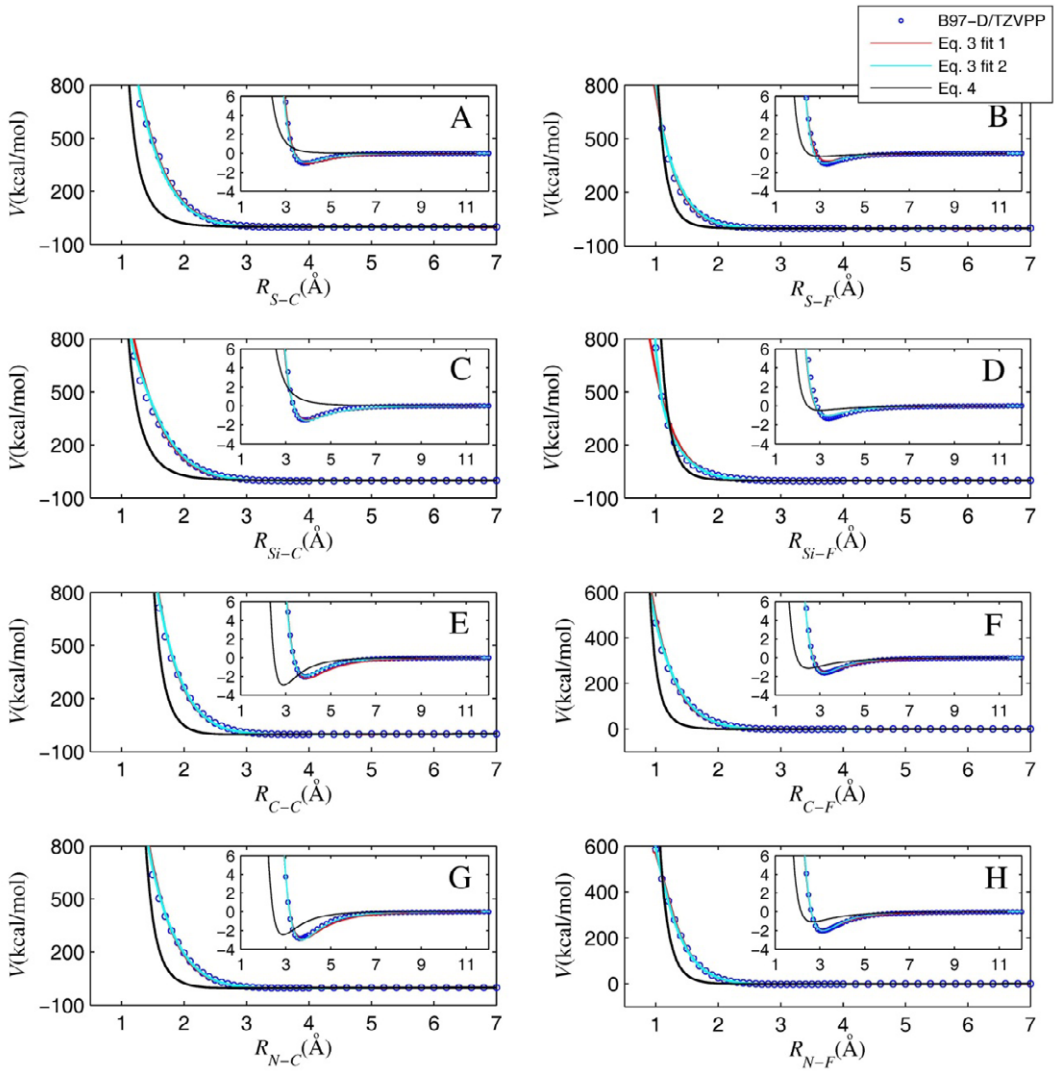

Figure 9

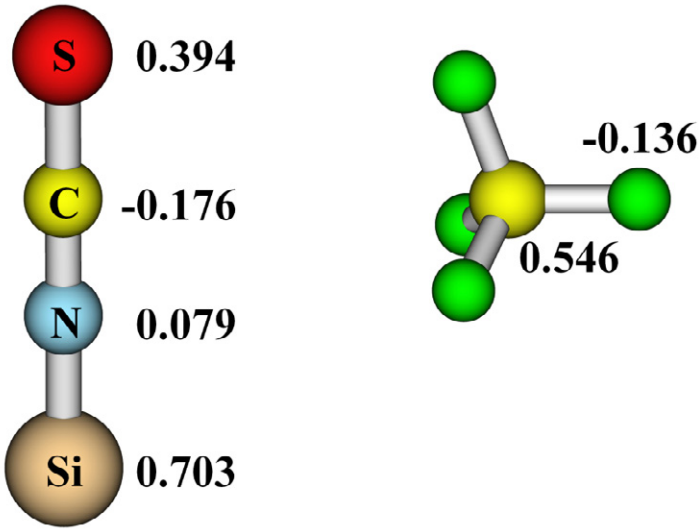

Figure 10

The figure shows intermolecular potential energy curves for interaction of $(CH_3)_2SiNCS^+$ with a model compound of perfluorinated self-assembled monolayers. The silyl ion is approaching the surface perpendicularly.

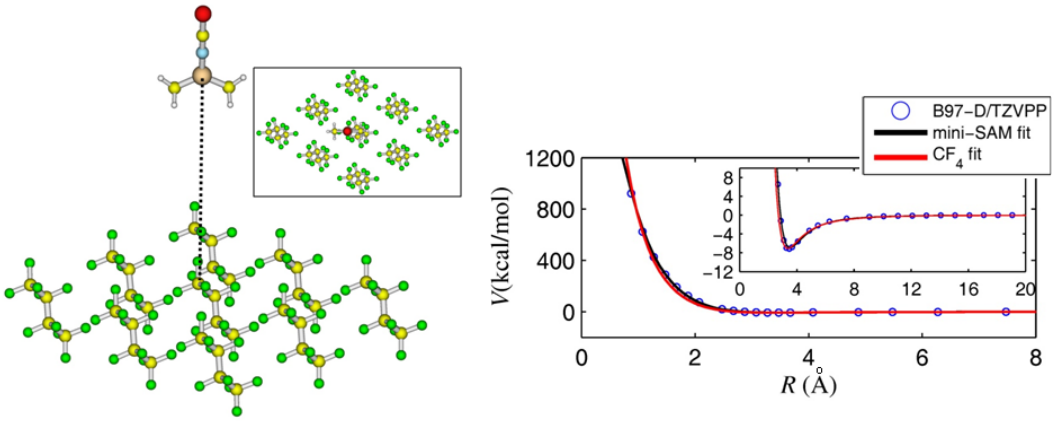

> Intermolecular potentials are developed for interactions of SiNCS+ and $(CH_3)_2SiNCS^+$ ions with perfluorinated self-assembled monolayers. > Pairwise potentials of the Buckingham type give good fits to intermolecular potential energy curves determined by DFT-D calculations. > Lennard-Jones potentials plus point-charge electrostatic terms give poor performance. > CF_4 is found to be a good model of an F-SAM surface for parameterization purposes.